

Measurement of the Branching Fraction and Photon Energy Moments of $B \rightarrow X_s \gamma$ and $A_{CP}(B \rightarrow X_{s+d} \gamma)$

B. Aubert,¹ R. Barate,¹ M. Bona,¹ D. Boutigny,¹ F. Couderc,¹ Y. Karyotakis,¹ J. P. Lees,¹ V. Poireau,¹
V. Tisserand,¹ A. Zghiche,¹ E. Grauges,² A. Palano,³ J. C. Chen,⁴ N. D. Qi,⁴ G. Rong,⁴ P. Wang,⁴ Y. S. Zhu,⁴
G. Eigen,⁵ I. Ofte,⁵ B. Stugu,⁵ G. S. Abrams,⁶ M. Battaglia,⁶ D. N. Brown,⁶ J. Button-Shafer,⁶ R. N. Cahn,⁶
E. Charles,⁶ M. S. Gill,⁶ Y. Groyzman,⁶ R. G. Jacobsen,⁶ J. A. Kadyk,⁶ L. T. Kerth,⁶ Yu. G. Kolomensky,⁶
G. Kukartsev,⁶ G. Lynch,⁶ L. M. Mir,⁶ P. J. Oddone,⁶ T. J. Orimoto,⁶ M. Pripstein,⁶ N. A. Roe,⁶ M. T. Ronan,⁶
W. A. Wenzel,⁶ P. del Amo Sanchez,⁷ M. Barrett,⁷ K. E. Ford,⁷ T. J. Harrison,⁷ A. J. Hart,⁷ C. M. Hawkes,⁷
S. E. Morgan,⁷ A. T. Watson,⁷ K. Goetzen,⁸ T. Held,⁸ H. Koch,⁸ B. Lewandowski,⁸ M. Pelizaeus,⁸ K. Peters,⁸
T. Schroeder,⁸ M. Steinke,⁸ J. T. Boyd,⁹ J. P. Burke,⁹ W. N. Cottingham,⁹ D. Walker,⁹ T. Cuhadar-Donszelmann,¹⁰
B. G. Fulsom,¹⁰ C. Hearty,¹⁰ N. S. Knecht,¹⁰ T. S. Mattison,¹⁰ J. A. McKenna,¹⁰ A. Khan,¹¹ P. Kyberd,¹¹
M. Saleem,¹¹ D. J. Sherwood,¹¹ L. Teodorescu,¹¹ V. E. Blinov,¹² A. D. Bukin,¹² V. P. Druzhinin,¹² V. B. Golubev,¹²
A. P. Onuchin,¹² S. I. Serednyakov,¹² Yu. I. Skovpen,¹² E. P. Solodov,¹² K. Yu Todyshev,¹² D. S. Best,¹³
M. Bondioli,¹³ M. Bruinsma,¹³ M. Chao,¹³ S. Curry,¹³ I. Eschrich,¹³ D. Kirkby,¹³ A. J. Lankford,¹³ P. Lund,¹³
M. Mandelkern,¹³ R. K. Mommsen,¹³ W. Roethel,¹³ D. P. Stoker,¹³ S. Abachi,¹⁴ C. Buchanan,¹⁴ S. D. Foulkes,¹⁵
J. W. Gary,¹⁵ O. Long,¹⁵ B. C. Shen,¹⁵ K. Wang,¹⁵ L. Zhang,¹⁵ H. K. Hadavand,¹⁶ E. J. Hill,¹⁶ H. P. Paar,¹⁶
S. Rahatlou,¹⁶ V. Sharma,¹⁶ J. W. Berryhill,¹⁷ C. Campagnari,¹⁷ A. Cunha,¹⁷ B. Dahmes,¹⁷ T. M. Hong,¹⁷
D. Kovalskiy,¹⁷ J. D. Richman,¹⁷ T. W. Beck,¹⁸ A. M. Eisner,¹⁸ C. J. Flacco,¹⁸ C. A. Heusch,¹⁸ J. Kroseberg,¹⁸
W. S. Lockman,¹⁸ G. Nesom,¹⁸ T. Schalk,¹⁸ R. E. Schmitz,¹⁸ B. A. Schumm,¹⁸ A. Seiden,¹⁸ P. Spradlin,¹⁸
D. C. Williams,¹⁸ M. G. Wilson,¹⁸ J. Albert,¹⁹ E. Chen,¹⁹ A. Dvoretzkii,¹⁹ F. Fang,¹⁹ D. G. Hitlin,¹⁹ I. Narsky,¹⁹
T. Piatenko,¹⁹ F. C. Porter,¹⁹ A. Ryd,¹⁹ A. Samuel,¹⁹ G. Mancinelli,²⁰ B. T. Meadows,²⁰ M. D. Sokoloff,²⁰
F. Blanc,²¹ P. C. Bloom,²¹ S. Chen,²¹ W. T. Ford,²¹ J. F. Hirschauer,²¹ A. Kreisel,²¹ U. Nauenberg,²¹ A. Olivas,²¹
W. O. Ruddick,²¹ J. G. Smith,²¹ K. A. Ulmer,²¹ S. R. Wagner,²¹ J. Zhang,²¹ A. Chen,²² E. A. Eckhart,²²
A. Soffer,²² W. H. Toki,²² R. J. Wilson,²² F. Winklmeier,²² Q. Zeng,²² D. D. Altenburg,²³ E. Feltresi,²³
A. Hauke,²³ H. Jasper,²³ A. Petzold,²³ B. Spaan,²³ T. Brandt,²⁴ V. Klose,²⁴ H. M. Lacker,²⁴ W. F. Mader,²⁴
R. Nogowski,²⁴ J. Schubert,²⁴ K. R. Schubert,²⁴ R. Schwierz,²⁴ J. E. Sundermann,²⁴ A. Volk,²⁴ D. Bernard,²⁵
G. R. Bonneaud,²⁵ P. Grenier,²⁵ * E. Latour,²⁵ Ch. Thiebaux,²⁵ M. Verderi,²⁵ D. J. Bard,²⁶ P. J. Clark,²⁶
W. Gradl,²⁶ F. Muheim,²⁶ S. Playfer,²⁶ A. I. Robertson,²⁶ Y. Xie,²⁶ M. Andreotti,²⁷ D. Bettoni,²⁷ C. Bozzi,²⁷
R. Calabrese,²⁷ G. Cibinetto,²⁷ E. Luppi,²⁷ M. Negrini,²⁷ A. Petrella,²⁷ L. Piemontese,²⁷ E. Prencipe,²⁷
F. Anulli,²⁸ R. Baldini-Ferrolì,²⁸ A. Calcaterra,²⁸ R. de Sangro,²⁸ G. Finocchiaro,²⁸ S. Pacetti,²⁸ P. Patteri,²⁸
I. M. Peruzzi,²⁸ † M. Piccolo,²⁸ M. Rama,²⁸ A. Zallo,²⁸ A. Buzzo,²⁹ R. Capra,²⁹ R. Contri,²⁹ M. Lo Vetere,²⁹
M. M. Macri,²⁹ M. R. Monge,²⁹ S. Passaggio,²⁹ C. Patrignani,²⁹ E. Robutti,²⁹ A. Santroni,²⁹ S. Tosi,²⁹
G. Brandenburg,³⁰ K. S. Chaisanguanthum,³⁰ M. Morii,³⁰ J. Wu,³⁰ R. S. Dubitzky,³¹ J. Marks,³¹ S. Schenk,³¹
U. Uwer,³¹ W. Bhimji,³² D. A. Bowerman,³² P. D. Dauncey,³² U. Egede,³² R. L. Flack,³² J. A. Nash,³²
M. B. Nikolich,³² W. Panduro Vazquez,³² X. Chai,³³ M. J. Charles,³³ U. Mallik,³³ N. T. Meyer,³³ V. Ziegler,³³
J. Cochran,³⁴ H. B. Crawley,³⁴ L. Dong,³⁴ V. Eyges,³⁴ W. T. Meyer,³⁴ S. Prell,³⁴ E. I. Rosenberg,³⁴ A. E. Rubin,³⁴
A. V. Gritsan,³⁵ M. Fritsch,³⁶ G. Schott,³⁶ N. Arnaud,³⁷ M. Davier,³⁷ G. Grosdidier,³⁷ A. Höcker,³⁷ F. Le
Diberder,³⁷ V. Lepeltier,³⁷ A. M. Lutz,³⁷ A. Oyanguren,³⁷ S. Pruvot,³⁷ S. Rodier,³⁷ P. Roudeau,³⁷ M. H. Schune,³⁷
A. Stocchi,³⁷ W. F. Wang,³⁷ G. Wormser,³⁷ C. H. Cheng,³⁸ D. J. Lange,³⁸ D. M. Wright,³⁸ C. A. Chavez,³⁹
I. J. Forster,³⁹ J. R. Fry,³⁹ E. Gabathuler,³⁹ R. Gamet,³⁹ K. A. George,³⁹ D. E. Hutchcroft,³⁹ D. J. Payne,³⁹
K. C. Schofield,³⁹ C. Touramanis,³⁹ A. J. Bevan,⁴⁰ F. Di Lodovico,⁴⁰ W. Menges,⁴⁰ R. Sacco,⁴⁰ G. Cowan,⁴¹
H. U. Flaecher,⁴¹ D. A. Hopkins,⁴¹ P. S. Jackson,⁴¹ T. R. McMahon,⁴¹ S. Ricciardi,⁴¹ F. Salvatore,⁴¹ A. C. Wren,⁴¹
D. N. Brown,⁴² C. L. Davis,⁴² J. Allison,⁴³ N. R. Barlow,⁴³ R. J. Barlow,⁴³ Y. M. Chia,⁴³ C. L. Edgar,⁴³
G. D. Lafferty,⁴³ M. T. Naisbit,⁴³ J. C. Williams,⁴³ J. I. Yi,⁴³ C. Chen,⁴⁴ W. D. Hulsbergen,⁴⁴ A. Jawahery,⁴⁴
C. K. Lae,⁴⁴ D. A. Roberts,⁴⁴ G. Simi,⁴⁴ G. Blaylock,⁴⁵ C. Dallapiccola,⁴⁵ S. S. Hertzbach,⁴⁵ X. Li,⁴⁵
T. B. Moore,⁴⁵ S. Saremi,⁴⁵ H. Staengle,⁴⁵ R. Cowan,⁴⁶ G. Sciolla,⁴⁶ S. J. Sekula,⁴⁶ M. Spitznagel,⁴⁶ F. Taylor,⁴⁶
R. K. Yamamoto,⁴⁶ H. Kim,⁴⁷ P. M. Patel,⁴⁷ S. H. Robertson,⁴⁷ A. Lazzaro,⁴⁸ V. Lombardo,⁴⁸ F. Palombo,⁴⁸

J. M. Bauer,⁴⁹ L. Cremaldi,⁴⁹ V. Eschenburg,⁴⁹ R. Godang,⁴⁹ R. Kroeger,⁴⁹ D. A. Sanders,⁴⁹ D. J. Summers,⁴⁹ H. W. Zhao,⁴⁹ S. Brunet,⁵⁰ D. Côté,⁵⁰ P. Taras,⁵⁰ F. B. Viaud,⁵⁰ H. Nicholson,⁵¹ N. Cavallo,^{52, †} G. De Nardo,⁵² F. Fabozzi,^{52, †} C. Gatto,⁵² L. Lista,⁵² D. Monorchio,⁵² P. Paolucci,⁵² D. Piccolo,⁵² C. Sciacca,⁵² M. Baak,⁵³ G. Raven,⁵³ H. L. Snoek,⁵³ C. P. Jessop,⁵⁴ J. M. LoSecco,⁵⁴ T. Allmendinger,⁵⁵ G. Benelli,⁵⁵ K. K. Gan,⁵⁵ K. Honscheid,⁵⁵ D. Hufnagel,⁵⁵ P. D. Jackson,⁵⁵ H. Kagan,⁵⁵ R. Kass,⁵⁵ A. M. Rahimi,⁵⁵ R. Ter-Antonyan,⁵⁵ Q. K. Wong,⁵⁵ N. L. Blount,⁵⁶ J. Brau,⁵⁶ R. Frey,⁵⁶ O. Igonkina,⁵⁶ M. Lu,⁵⁶ C. T. Potter,⁵⁶ R. Rahmat,⁵⁶ N. B. Sinev,⁵⁶ D. Strom,⁵⁶ J. Strube,⁵⁶ E. Torrence,⁵⁶ F. Galeazzi,⁵⁷ A. Gaz,⁵⁷ M. Margoni,⁵⁷ M. Morandin,⁵⁷ A. Pompili,⁵⁷ M. Posocco,⁵⁷ M. Rotondo,⁵⁷ F. Simonetto,⁵⁷ R. Stroili,⁵⁷ C. Voci,⁵⁷ M. Benayoun,⁵⁸ J. Chauveau,⁵⁸ P. David,⁵⁸ L. Del Buono,⁵⁸ Ch. de la Vaissière,⁵⁸ O. Hamon,⁵⁸ B. L. Hartfiel,⁵⁸ M. J. J. John,⁵⁸ J. Malclès,⁵⁸ J. Ocariz,⁵⁸ L. Roos,⁵⁸ G. Therin,⁵⁸ P. K. Behera,⁵⁹ L. Gladney,⁵⁹ J. Panetta,⁵⁹ M. Biasini,⁶⁰ R. Covarelli,⁶⁰ C. Angelini,⁶¹ G. Batignani,⁶¹ S. Bettarini,⁶¹ F. Bucci,⁶¹ G. Calderini,⁶¹ M. Carpinelli,⁶¹ R. Cenci,⁶¹ F. Forti,⁶¹ M. A. Giorgi,⁶¹ A. Lusiani,⁶¹ G. Marchiori,⁶¹ M. A. Mazur,⁶¹ M. Morganti,⁶¹ N. Neri,⁶¹ E. Paoloni,⁶¹ G. Rizzo,⁶¹ J. J. Walsh,⁶¹ M. Haire,⁶² D. Judd,⁶² D. E. Wagoner,⁶² J. Biesiada,⁶³ N. Danielson,⁶³ P. Elmer,⁶³ Y. P. Lau,⁶³ C. Lu,⁶³ J. Olsen,⁶³ A. J. S. Smith,⁶³ A. V. Telnov,⁶³ F. Bellini,⁶⁴ G. Cavoto,⁶⁴ A. D’Orazio,⁶⁴ D. del Re,⁶⁴ E. Di Marco,⁶⁴ R. Faccini,⁶⁴ F. Ferrarotto,⁶⁴ F. Ferroni,⁶⁴ M. Gaspero,⁶⁴ L. Li Gioi,⁶⁴ M. A. Mazzoni,⁶⁴ S. Morganti,⁶⁴ G. Piredda,⁶⁴ F. Polci,⁶⁴ F. Safai Tehrani,⁶⁴ C. Voena,⁶⁴ M. Ebert,⁶⁵ H. Schröder,⁶⁵ R. Waldi,⁶⁵ T. Adye,⁶⁶ N. De Groot,⁶⁶ B. Franek,⁶⁶ E. O. Olaiya,⁶⁶ F. F. Wilson,⁶⁶ R. Aleksan,⁶⁷ S. Emery,⁶⁷ A. Gaidot,⁶⁷ S. F. Ganzhur,⁶⁷ G. Hamel de Monchenault,⁶⁷ W. Kozanecki,⁶⁷ M. Legendre,⁶⁷ G. Vasseur,⁶⁷ Ch. Yèche,⁶⁷ M. Zito,⁶⁷ X. R. Chen,⁶⁸ H. Liu,⁶⁸ W. Park,⁶⁸ M. V. Purohit,⁶⁸ J. R. Wilson,⁶⁸ M. T. Allen,⁶⁹ D. Aston,⁶⁹ R. Bartoldus,⁶⁹ P. Bechtle,⁶⁹ N. Berger,⁶⁹ R. Claus,⁶⁹ J. P. Coleman,⁶⁹ M. R. Convery,⁶⁹ M. Cristinziani,⁶⁹ J. C. Dingfelder,⁶⁹ J. Dorfan,⁶⁹ G. P. Dubois-Felsmann,⁶⁹ D. Dujmic,⁶⁹ W. Dunwoodie,⁶⁹ R. C. Field,⁶⁹ T. Glanzman,⁶⁹ S. J. Gowdy,⁶⁹ M. T. Graham,⁶⁹ V. Halyo,⁶⁹ C. Hast,⁶⁹ T. Hryn’ova,⁶⁹ W. R. Innes,⁶⁹ M. H. Kelsey,⁶⁹ P. Kim,⁶⁹ D. W. G. S. Leith,⁶⁹ S. Li,⁶⁹ J. Libby,⁶⁹ S. Luitz,⁶⁹ V. Luth,⁶⁹ H. L. Lynch,⁶⁹ D. B. MacFarlane,⁶⁹ H. Marsiske,⁶⁹ R. Messner,⁶⁹ D. R. Muller,⁶⁹ C. P. O’Grady,⁶⁹ V. E. Ozcan,⁶⁹ A. Perazzo,⁶⁹ M. Perl,⁶⁹ T. Pulliam,⁶⁹ B. N. Ratcliff,⁶⁹ A. Roodman,⁶⁹ A. A. Salnikov,⁶⁹ R. H. Schindler,⁶⁹ J. Schwiening,⁶⁹ A. Snyder,⁶⁹ J. Stelzer,⁶⁹ D. Su,⁶⁹ M. K. Sullivan,⁶⁹ K. Suzuki,⁶⁹ S. K. Swain,⁶⁹ J. M. Thompson,⁶⁹ J. S. Tinslay,⁶⁹ J. Va’vra,⁶⁹ N. van Bakel,⁶⁹ M. Weaver,⁶⁹ A. J. R. Weinstein,⁶⁹ W. J. Wisniewski,⁶⁹ M. Wittgen,⁶⁹ D. H. Wright,⁶⁹ A. K. Yarritu,⁶⁹ K. Yi,⁶⁹ C. C. Young,⁶⁹ P. R. Burchat,⁷⁰ A. J. Edwards,⁷⁰ S. A. Majewski,⁷⁰ B. A. Petersen,⁷⁰ C. Roat,⁷⁰ L. Wilden,⁷⁰ S. Ahmed,⁷¹ M. S. Alam,⁷¹ R. Bula,⁷¹ J. A. Ernst,⁷¹ V. Jain,⁷¹ B. Pan,⁷¹ M. A. Saeed,⁷¹ F. R. Wappler,⁷¹ S. B. Zain,⁷¹ W. Bugg,⁷² M. Krishnamurthy,⁷² S. M. Spanier,⁷² R. Eckmann,⁷³ J. L. Ritchie,⁷³ A. Satpathy,⁷³ C. J. Schilling,⁷³ R. F. Schwitters,⁷³ J. M. Izen,⁷⁴ X. C. Lou,⁷⁴ S. Ye,⁷⁴ F. Bianchi,⁷⁵ F. Gallo,⁷⁵ D. Gamba,⁷⁵ M. Bomben,⁷⁶ L. Bosisio,⁷⁶ C. Cartaro,⁷⁶ F. Cossutti,⁷⁶ G. Della Ricca,⁷⁶ S. Dittongo,⁷⁶ L. Lanceri,⁷⁶ L. Vitale,⁷⁶ V. Azzolini,⁷⁷ F. Martinez-Vidal,⁷⁷ Sw. Banerjee,⁷⁸ B. Bhuyan,⁷⁸ C. M. Brown,⁷⁸ D. Fortin,⁷⁸ K. Hamano,⁷⁸ R. Kowalewski,⁷⁸ I. M. Nugent,⁷⁸ J. M. Roney,⁷⁸ R. J. Sobie,⁷⁸ J. J. Back,⁷⁹ P. F. Harrison,⁷⁹ T. E. Latham,⁷⁹ G. B. Mohanty,⁷⁹ M. Pappagallo,⁷⁹ H. R. Band,⁸⁰ X. Chen,⁸⁰ B. Cheng,⁸⁰ S. Dasu,⁸⁰ M. Datta,⁸⁰ K. T. Flood,⁸⁰ J. J. Hollar,⁸⁰ P. E. Kutter,⁸⁰ B. Mellado,⁸⁰ A. Mihalyi,⁸⁰ Y. Pan,⁸⁰ M. Pierini,⁸⁰ R. Prepost,⁸⁰ S. L. Wu,⁸⁰ Z. Yu,⁸⁰ and H. Neal⁸¹

(The BABAR Collaboration)

¹Laboratoire de Physique des Particules, F-74941 Annecy-le-Vieux, France

²Universitat de Barcelona, Facultat de Fisica Dept. ECM, E-08028 Barcelona, Spain

³Università di Bari, Dipartimento di Fisica and INFN, I-70126 Bari, Italy

⁴Institute of High Energy Physics, Beijing 100039, China

⁵University of Bergen, Institute of Physics, N-5007 Bergen, Norway

⁶Lawrence Berkeley National Laboratory and University of California, Berkeley, California 94720, USA

⁷University of Birmingham, Birmingham, B15 2TT, United Kingdom

⁸Ruhr Universität Bochum, Institut für Experimentalphysik 1, D-44780 Bochum, Germany

⁹University of Bristol, Bristol BS8 1TL, United Kingdom

¹⁰University of British Columbia, Vancouver, British Columbia, Canada V6T 1Z1

¹¹Brunel University, Uxbridge, Middlesex UB8 3PH, United Kingdom

¹²Budker Institute of Nuclear Physics, Novosibirsk 630090, Russia

¹³University of California at Irvine, Irvine, California 92697, USA

¹⁴University of California at Los Angeles, Los Angeles, California 90024, USA

¹⁵University of California at Riverside, Riverside, California 92521, USA

¹⁶University of California at San Diego, La Jolla, California 92093, USA

- ¹⁷University of California at Santa Barbara, Santa Barbara, California 93106, USA
- ¹⁸University of California at Santa Cruz, Institute for Particle Physics, Santa Cruz, California 95064, USA
- ¹⁹California Institute of Technology, Pasadena, California 91125, USA
- ²⁰University of Cincinnati, Cincinnati, Ohio 45221, USA
- ²¹University of Colorado, Boulder, Colorado 80309, USA
- ²²Colorado State University, Fort Collins, Colorado 80523, USA
- ²³Universität Dortmund, Institut für Physik, D-44221 Dortmund, Germany
- ²⁴Technische Universität Dresden, Institut für Kern- und Teilchenphysik, D-01062 Dresden, Germany
- ²⁵Ecole Polytechnique, Laboratoire Leprince-Ringuet, F-91128 Palaiseau, France
- ²⁶University of Edinburgh, Edinburgh EH9 3JZ, United Kingdom
- ²⁷Università di Ferrara, Dipartimento di Fisica and INFN, I-44100 Ferrara, Italy
- ²⁸Laboratori Nazionali di Frascati dell'INFN, I-00044 Frascati, Italy
- ²⁹Università di Genova, Dipartimento di Fisica and INFN, I-16146 Genova, Italy
- ³⁰Harvard University, Cambridge, Massachusetts 02138, USA
- ³¹Universität Heidelberg, Physikalisches Institut, Philosophenweg 12, D-69120 Heidelberg, Germany
- ³²Imperial College London, London, SW7 2AZ, United Kingdom
- ³³University of Iowa, Iowa City, Iowa 52242, USA
- ³⁴Iowa State University, Ames, Iowa 50011-3160, USA
- ³⁵Johns Hopkins University, Baltimore, Maryland 21218, USA
- ³⁶Universität Karlsruhe, Institut für Experimentelle Kernphysik, D-76021 Karlsruhe, Germany
- ³⁷Laboratoire de l'Accélérateur Linéaire, IN2P3-CNRS et Université Paris-Sud 11, Centre Scientifique d'Orsay, B.P. 34, F-91898 ORSAY Cedex, France
- ³⁸Lawrence Livermore National Laboratory, Livermore, California 94550, USA
- ³⁹University of Liverpool, Liverpool L69 7ZE, United Kingdom
- ⁴⁰Queen Mary, University of London, E1 4NS, United Kingdom
- ⁴¹University of London, Royal Holloway and Bedford New College, Egham, Surrey TW20 0EX, United Kingdom
- ⁴²University of Louisville, Louisville, Kentucky 40292, USA
- ⁴³University of Manchester, Manchester M13 9PL, United Kingdom
- ⁴⁴University of Maryland, College Park, Maryland 20742, USA
- ⁴⁵University of Massachusetts, Amherst, Massachusetts 01003, USA
- ⁴⁶Massachusetts Institute of Technology, Laboratory for Nuclear Science, Cambridge, Massachusetts 02139, USA
- ⁴⁷McGill University, Montréal, Québec, Canada H3A 2T8
- ⁴⁸Università di Milano, Dipartimento di Fisica and INFN, I-20133 Milano, Italy
- ⁴⁹University of Mississippi, University, Mississippi 38677, USA
- ⁵⁰Université de Montréal, Physique des Particules, Montréal, Québec, Canada H3C 3J7
- ⁵¹Mount Holyoke College, South Hadley, Massachusetts 01075, USA
- ⁵²Università di Napoli Federico II, Dipartimento di Scienze Fisiche and INFN, I-80126, Napoli, Italy
- ⁵³NIKHEF, National Institute for Nuclear Physics and High Energy Physics, NL-1009 DB Amsterdam, The Netherlands
- ⁵⁴University of Notre Dame, Notre Dame, Indiana 46556, USA
- ⁵⁵Ohio State University, Columbus, Ohio 43210, USA
- ⁵⁶University of Oregon, Eugene, Oregon 97403, USA
- ⁵⁷Università di Padova, Dipartimento di Fisica and INFN, I-35131 Padova, Italy
- ⁵⁸Universités Paris VI et VII, Laboratoire de Physique Nucléaire et de Hautes Energies, F-75252 Paris, France
- ⁵⁹University of Pennsylvania, Philadelphia, Pennsylvania 19104, USA
- ⁶⁰Università di Perugia, Dipartimento di Fisica and INFN, I-06100 Perugia, Italy
- ⁶¹Università di Pisa, Dipartimento di Fisica, Scuola Normale Superiore and INFN, I-56127 Pisa, Italy
- ⁶²Prairie View A&M University, Prairie View, Texas 77446, USA
- ⁶³Princeton University, Princeton, New Jersey 08544, USA
- ⁶⁴Università di Roma La Sapienza, Dipartimento di Fisica and INFN, I-00185 Roma, Italy
- ⁶⁵Universität Rostock, D-18051 Rostock, Germany
- ⁶⁶Rutherford Appleton Laboratory, Chilton, Didcot, Oxon, OX11 0QX, United Kingdom
- ⁶⁷DSM/Dapnia, CEA/Saclay, F-91191 Gif-sur-Yvette, France
- ⁶⁸University of South Carolina, Columbia, South Carolina 29208, USA
- ⁶⁹Stanford Linear Accelerator Center, Stanford, California 94309, USA
- ⁷⁰Stanford University, Stanford, California 94305-4060, USA
- ⁷¹State University of New York, Albany, New York 12222, USA
- ⁷²University of Tennessee, Knoxville, Tennessee 37996, USA
- ⁷³University of Texas at Austin, Austin, Texas 78712, USA
- ⁷⁴University of Texas at Dallas, Richardson, Texas 75083, USA
- ⁷⁵Università di Torino, Dipartimento di Fisica Sperimentale and INFN, I-10125 Torino, Italy
- ⁷⁶Università di Trieste, Dipartimento di Fisica and INFN, I-34127 Trieste, Italy
- ⁷⁷IFIC, Universitat de Valencia-CSIC, E-46071 Valencia, Spain
- ⁷⁸University of Victoria, Victoria, British Columbia, Canada V8W 3P6
- ⁷⁹Department of Physics, University of Warwick, Coventry CV4 7AL, United Kingdom

⁸⁰University of Wisconsin, Madison, Wisconsin 53706, USA

⁸¹Yale University, New Haven, Connecticut 06511, USA

(Dated: September 12, 2018)

The photon spectrum in $B \rightarrow X_s \gamma$ decay, where X_s is any strange hadronic state, is studied using a data sample of $88.5 \times 10^6 e^+e^- \rightarrow \Upsilon(4S) \rightarrow B\bar{B}$ decays collected by the BABAR experiment at SLAC. The partial branching fraction, $\Delta\mathcal{B}(B \rightarrow X_s \gamma) = (3.67 \pm 0.29(stat.) \pm 0.34(sys.) \pm 0.29(model)) \times 10^{-4}$, the first moment $\langle E_\gamma \rangle = 2.288 \pm 0.025 \pm 0.017 \pm 0.015$ GeV and the second moment $\langle E_\gamma^2 \rangle = 0.0328 \pm 0.0040 \pm 0.0023 \pm 0.0036$ GeV² are measured for the photon energy range $1.9 \text{ GeV} < E_\gamma < 2.7 \text{ GeV}$. They are also measured for narrower E_γ ranges. The moments are then fit to recent theoretical calculations to extract the Heavy Quark Expansion parameters, m_b and μ_π^2 , and to extrapolate the partial branching fraction to $E_\gamma > 1.6$ GeV. In addition, the direct CP asymmetry $A_{CP}(B \rightarrow X_{s+d}\gamma)$ is measured to be $-0.110 \pm 0.115(stat.) \pm 0.017(sys.)$.

PACS numbers: 13.25.Hw, 12.15.Hh, 11.30.Er

In the Standard Model (SM) the radiative decay of the b quark, $b \rightarrow s\gamma$, proceeds via a loop diagram, and is sensitive to possible new physics, with new heavy particles participating in the loop [1]. Next-to-leading-order SM calculations for the branching fraction give $\mathcal{B}(B \rightarrow X_s \gamma) = (3.61_{-0.49}^{+0.37}) \times 10^{-4}$ ($E_\gamma > 1.6$ GeV) [2], and calculations to higher order, which are expected to considerably decrease the uncertainty, are currently underway [3]. The shape of the photon energy spectrum, which is insensitive to non-SM physics [4], can be used to determine the Heavy Quark Expansion (HQE) parameters, m_b and μ_π^2 [5, 6], related to the mass and momentum of the b quark within the B meson. These parameters can be used to reduce the error in the extraction of the CKM matrix elements $|V_{cb}|$ and $|V_{ub}|$ from semi-leptonic B -meson decays [7]. New physics can also significantly enhance the direct CP asymmetry for $b \rightarrow s\gamma$ and $b \rightarrow d\gamma$ decay [2], $A_{CP} = \frac{\Gamma(b \rightarrow s\gamma + b \rightarrow d\gamma) - \Gamma(\bar{b} \rightarrow \bar{s}\gamma + \bar{b} \rightarrow \bar{d}\gamma)}{\Gamma(b \rightarrow s\gamma + b \rightarrow d\gamma) + \Gamma(\bar{b} \rightarrow \bar{s}\gamma + \bar{b} \rightarrow \bar{d}\gamma)}$ which is $\approx 10^{-9}$ in the SM [8]. Measurements of this joint asymmetry complement those of A_{CP} in $b \rightarrow s\gamma$ [9] to constrain new physics models.

This letter reports on a fully-inclusive analysis of $B \rightarrow X_s \gamma$ decays collected from $e^+e^- \rightarrow \Upsilon(4S) \rightarrow B\bar{B}$, where the photon from the decay of one B meson is measured, but the X_s is not reconstructed. This avoids incurring large uncertainties from the modeling of the X_s fragmentation, but at the cost of high backgrounds which need to be strongly suppressed. The principal backgrounds are from other $B\bar{B}$ decays containing a high energy photon and from continuum $q\bar{q}$ ($q = u, d, s, c$) and $\tau^+\tau^-$ events. The continuum background, including a contribution from initial state radiation (ISR), is suppressed principally by requiring a high-momentum lepton from the non-signal B decay, and also by discriminating against its more jet-like topology. The $B\bar{B}$ background to high energy photons, dominated by π^0 and η decays, is reduced by vetoing on reconstructed π^0 or η . The residual continuum background is subtracted using off-resonance data taken at a center-of-mass energy 40 MeV below that of the $\Upsilon(4S)$, while the remaining $B\bar{B}$ background is estimated using a Monte Carlo simulation which has been checked and

corrected using data control samples. Previous inclusive measurements of $B \rightarrow X_s \gamma$ have been presented by the CLEO [10], BELLE [11] and BABAR [12] collaborations using alternative techniques which incur different systematic uncertainties.

The results presented are based on data collected with the BABAR detector [13] at the PEP-II asymmetric-energy e^+e^- collider located at the Stanford Linear Accelerator Center. The on-resonance integrated luminosity is 81.5 fb^{-1} , corresponding to 88.5 million $B\bar{B}$ events. Additionally, 9.6 fb^{-1} of off-resonance data are used in the continuum background subtraction. The BABAR Monte Carlo simulation program, based on GEANT4 [14], EVTGEN [15] and JETSET [16], is used to generate samples of B^+B^- and $B^0\bar{B}^0$ (excluding signal channels), $q\bar{q}$, $\tau^+\tau^-$, and signal events. The signal models used to calculate efficiencies are based on references [5] (“kinetic scheme”) and [6] (“shape function scheme”) and on an earlier calculation [4] (“KN”). These predictions approximate the X_s resonance structure with a smooth distribution in m_{X_s} . This is reasonable except at the lowest masses where the $K^*(892)$ dominates the spectrum. Hence the portion of the m_{X_s} spectrum below $1.1 \text{ GeV}/c^2$ is replaced by a Breit-Wigner $K^*(892)$ distribution. The analysis was done “blind” in the range of reconstructed photon energy E_γ^* from 1.9 to 2.9 GeV (asterisk denotes the $\Upsilon(4S)$ rest frame); that is, the on-resonance data were not looked at until all selection requirements were set and the corrected backgrounds determined. The signal range is limited by high $B\bar{B}$ backgrounds at low E_γ^* .

The event selection begins by finding at least one photon candidate with, $1.6 < E_\gamma^* < 3.4$ GeV, in the event. A photon candidate is a localized electromagnetic calorimeter energy deposit with a lateral profile consistent with that of a single photon. It is required to be isolated by 25 cm from any other energy deposit and to be well contained in the calorimeter ($-0.74 < \cos\theta_\gamma < 0.93$), where θ_γ is the polar angle with respect to the beam-axis. Photons that are consistent with originating from an identifiable π^0 or $\eta \rightarrow \gamma\gamma$ decay are vetoed. Hadronic events are

selected by requiring at least three reconstructed charged particles and the normalized second Fox-Wolfram moment R_2^* to be less than 0.55. To reduce radiative Bhabha and two-photon backgrounds, the number of charged particles plus half the number of photons with energy above 0.08 GeV is required to be ≥ 4.5 .

Event shape variables are used to exploit the difference in topology of isotropic $B\bar{B}$ events and jet-like continuum events. This is accomplished by the R_2^* requirement as well as a single linear discriminant formed from nineteen different variables. Eighteen of the quantities are the sum of charged and neutral energy found in 10-degree cones (from 0 to 180 degrees) centered on the photon candidate direction; the photon energy is not included. Additionally the discriminant includes R_2'/R_2^* , where R_2' is the normalized second Fox-Wolfram moment calculated in the frame recoiling against the photon, which for ISR events is the $q\bar{q}$ rest frame. The discriminant coefficients were determined by maximizing the separation power between simulated signal and continuum events.

Lepton tagging further reduces the backgrounds from continuum events. About 20% of B mesons decay semi-leptonically to either e or μ . Leptons from hadron decays in continuum events tend to be at lower momentum. Since the tag lepton comes from the recoiling B meson, it does not compromise the inclusiveness of the $B \rightarrow X_s \gamma$ selection. The tag lepton is required to have momentum $p_e^* > 1.25$ GeV/ c for electrons and $p_\mu^* > 1.5$ GeV/ c for muons. Additionally requiring the photon-lepton angle, $\cos\theta_{\gamma\ell}^* > -0.7$ removes more continuum background, in which the lepton and photon candidates tend to be back-to-back. Finally the presence of a relatively high-energy neutrino in semi-leptonic B decays is exploited by requiring the missing energy of the event, $E_{\text{miss}}^* > 0.8$ GeV/ c . Virtually all of the tagging leptons arise from the decay $B \rightarrow X_c \ell \nu$. The rate of such events in the simulation is corrected as a function of lepton momentum [17].

The event selection is chosen to maximize the statistical significance of the expected signal using simulated signal (KN with $m_b = 4.80$ GeV/ c^2 , $\mu_\pi^2 = 0.30$ GeV 2) and background events, allowing for the low statistics of the off-resonance data used for the subtraction of continuum background. After selection the low energy range, $1.6 < E_\gamma^* < 1.9$ GeV, is dominated by the $B\bar{B}$ background, while the high energy range, $2.9 < E_\gamma^* < 3.4$ GeV, is dominated by the continuum background; they provide control regions for the $B\bar{B}$ subtraction and continuum subtraction, respectively. The signal region lies between 1.9 GeV and 2.7 GeV. The signal efficiency ($\approx 1.6\%$ for this E_γ^* range) depends on E_γ^* and the signal model, but has negligible dependence on the details of the fragmentation of the X_s .

The $B\bar{B}$ background is estimated with the simulated $B\bar{B}$ data set. It consists predominantly of photons originating from π^0 or η decays ($\approx 80\%$). Other significant sources are $\bar{\pi}$'s which fake photons by annihilating in the

calorimeter and electrons that are misreconstructed or lost, or that undergo hard Bremsstrahlung. The $\pi^0(\eta)$ background simulation is compared to data by using the same selection criteria as for $B \rightarrow X_s \gamma$ but removing the $\pi^0(\eta)$ vetos. The photon energy and lepton momentum thresholds are relaxed to $E_\gamma^* > 1.0$ GeV, $p_e^* > 1.0$ GeV/ c , $p_\mu^* > 1.1$ GeV/ c to gain statistics. The yields of $\pi^0(\eta)$ are measured in bins of $E_{\pi^0(\eta)}^*$ by fitting the $\gamma\gamma$ mass distributions in on-resonance data, off-resonance data and simulated $B\bar{B}$ background. Correction factors to the $\pi^0(\eta)$ components of the $B\bar{B}$ simulation are derived from these yields, including a small adjustment for the different efficiencies of the $\pi^0(\eta)$ vetoes between data and simulation. As no $\bar{\pi}$ control sample could be isolated, this source of $B\bar{B}$ background is corrected by comparing in data and simulation the inclusive \bar{p} yields in B decay and the calorimeter response to \bar{p} 's, using a $\bar{\Lambda} \rightarrow \bar{p}\pi^+$ sample. The electron component of the $B\bar{B}$ simulation is corrected with electrons from a Bhabha data sample, taking into account the lower track multiplicity of these events compared to the signal events. Finally, the small contributions from ω and η' decays are corrected using inclusive B decay data. After including all corrections and systematic errors the expected background yield from the simulation in the $B\bar{B}$ control region ($1.6 < E_\gamma^* < 1.9$ GeV) is 1667 ± 54 events, compared to 1790 ± 64 events observed in data after continuum subtraction. Note that a small contribution in this region from the expected signal (≈ 20 to 40 events) has been neglected in this comparison. In the high energy control region $2.9 < E_\gamma^* < 3.4$ GeV the expected background is 390 ± 20 events, compared to 393 ± 58 events observed in data.

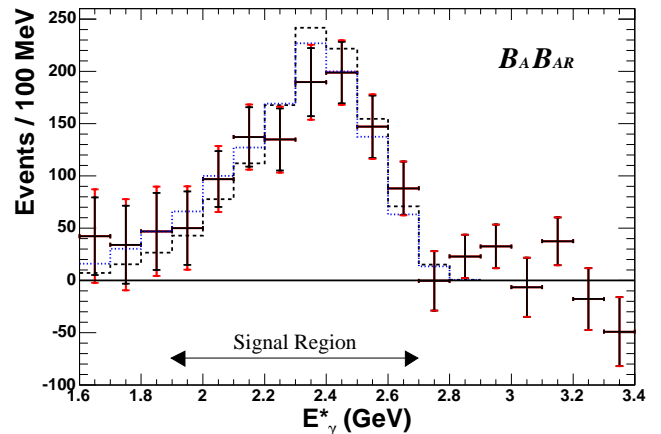


FIG. 1: The photon energy spectrum after background subtraction, uncorrected for efficiency. The inner error bars are statistical and the outer include systematic errors added in quadrature. The histograms show the spectra for values of m_b and μ_π^2 from the best fits to the moments in the kinetic scheme (dashed) and shape function scheme (dotted), normalized to the data in the signal region.

Figure 1 shows the measured spectrum for signal and

TABLE I: The measured partial branching fraction, first and second moment ($\pm stat. \pm syst. \pm model$) for different ranges of E_γ in the B rest frame.

E_γ (GeV)	$\Delta\mathcal{B}(B \rightarrow X_s\gamma)$ (10^{-4})	$\langle E_\gamma \rangle$ (GeV)	$\langle E_\gamma^2 \rangle - \langle E_\gamma \rangle^2$ (GeV^2)
1.9 to 2.7	$3.67 \pm 0.29 \pm 0.34 \pm 0.29$	$2.288 \pm 0.025 \pm 0.017 \pm 0.015$	$0.0328 \pm 0.0040 \pm 0.0023 \pm 0.0036$
2.0 to 2.7	$3.41 \pm 0.27 \pm 0.29 \pm 0.23$	$2.316 \pm 0.016 \pm 0.010 \pm 0.013$	$0.0266 \pm 0.0026 \pm 0.0010 \pm 0.0020$
2.1 to 2.7	$2.97 \pm 0.24 \pm 0.25 \pm 0.17$	$2.355 \pm 0.014 \pm 0.007 \pm 0.011$	$0.0191 \pm 0.0019 \pm 0.0006 \pm 0.0015$
2.2 to 2.7	$2.42 \pm 0.21 \pm 0.20 \pm 0.13$	$2.407 \pm 0.012 \pm 0.005 \pm 0.008$	$0.0116 \pm 0.0014 \pm 0.0004 \pm 0.0005$

control regions after the $B\bar{B}$ and continuum backgrounds have been subtracted. To extract partial branching fractions (PBFs) and first and second moments from this spectrum it is necessary to first correct for efficiency. Theoretical predictions are made for the true E_γ in the B meson rest frame, whereas the experimental measurements are made with reconstructed E_γ^* in the $\Upsilon(4S)$ frame. Hence it is also necessary to correct for smearing due to the asymmetric calorimeter resolution and the Doppler shift between the $\Upsilon(4S)$ frame and the B rest frame. The efficiency and smearing corrections depend upon the assumed signal model (underlying theory and parameter values). In a broad selection of signal models it is found that the efficiency for each E_γ^* range has a model-independent linear relationship to the mean E_γ^* in that range. Hence a nominal signal model is chosen for which the mean matches the data, and a model-dependence uncertainty is assigned to the PBFs and moments based on signal models within one (statistical and systematic) standard deviation of the measured mean E_γ^* . To correct for resolution smearing a small multiplicative correction to the PBF and small additive corrections to the first and second moments are computed using the nominal signal model, and an uncertainty assigned based on a conservative range of models. The model-dependence uncertainty from the smearing correction is fully correlated with the corresponding uncertainty of the efficiency correction.

The results for four energy ranges are given in Table 1 along with the statistical, systematic and model errors. The PBFs have been corrected to exclude a $(4.0 \pm 0.4)\%$ [2, 18] contribution from $b \rightarrow d\gamma$. The systematic errors are described below and the associated correlation matrices are given in the appendix.

The most significant systematic uncertainty in the measurement of the spectrum is from the uncertainty in the corrections to the $B\bar{B}$ background simulation. It is due mostly to the statistical uncertainty on the correction factors derived from the $\pi^0(\eta)$ control sample. The $B\bar{B}$ corrections depend on E_γ^* ; the resulting correlations between the 100 MeV E_γ^* bins have been taken into account in the computation of the total systematic uncertainty in the PBFs and moments. For example, for $2.0 \text{ GeV} < E_\gamma < 2.7 \text{ GeV}$, the $B\bar{B}$ corrections contribute 5.5% to a total systematic uncertainty of 8.5% of the PBF, and 0.008 GeV and 0.0009 GeV^2 of the total

systematic uncertainty of the first and second moments, respectively. Additional contributions to the PBF uncertainty (added in quadrature), all energy-independent, come from the photon selection (3.3%) due to the photon efficiency, determined with π^0 's from τ decay, and the isolation requirement, calorimeter energy scale and resolution, determined from $B \rightarrow K^*\gamma$ decays and photons from virtual Compton scattering; efficiency of the event shape variable selection (3%), determined from a π^0 control sample; the semi-leptonic corrections (3%); lepton identification (2%) and the modeling of the X_s fragmentation (1.5%). Additional uncertainties to the first and second moment, added in quadrature, come from the uncertainty in the calorimeter energy scale (0.006 GeV) and resolution (0.0004 GeV^2), respectively.

The parameters m_b and μ_π^2 , which are defined differently in the kinetic (K) and shape function (SF) schemes, can be extracted by fitting theoretical predictions to the measured moments. The first moments for $E_\gamma > 1.9$ and 2.0 GeV and the second moment for $E_\gamma > 2.0$ GeV are fitted, taking into account the correlations between the measured moments. As the moments are dependent on the assumed signal model due to the efficiency and resolution smearing corrections, the signal model and the model-dependence errors are adjusted based on the results of the fit and the moments are recomputed and refit. Only a few iterations are required until the result is stable. In the kinetic scheme $m_{b(K)} = 4.44_{-0.07}^{+0.08+0.12} \text{ GeV}/c^2$ and $\mu_{\pi(K)}^2 = 0.64_{-0.12-0.24}^{+0.13+0.23} \text{ GeV}^2$, with a correlation of -0.93 . The first error is due to the uncertainty in the measured moments and the second error is due to uncertainty in the theoretical calculations [5]. In the shape function scheme, using the exponential shape function form [6], $m_{b(SF)} = 4.43_{-0.08}^{+0.07} \text{ GeV}/c^2$ and $\mu_{\pi(SF)}^2 = 0.44_{-0.07}^{+0.06} \text{ GeV}^2$, with a correlation of -0.63 . If the Gaussian shape function form were used, $m_{b(SF)}$ and $\mu_{\pi(SF)}^2$ would increase by 0.13 GeV/c^2 and 0.01 GeV^2 , respectively. The spectra with the fitted parameters are compared to data in figure 1. These results (without theory error) are then used to extrapolate the measured partial branching fraction from $E_\gamma > 1.9$ GeV to 1.6 GeV to allow comparisons to theoretical predictions. In the kinetic scheme $\mathcal{B}(B \rightarrow X_s\gamma, E_\gamma > 1.6 \text{ GeV}) = (3.94 \pm 0.31 \pm 0.36 \pm 0.21) \times 10^{-4}$ and in the shape function scheme $\mathcal{B}(B \rightarrow X_s\gamma, E_\gamma > 1.6 \text{ GeV}) = (4.79 \pm 0.38 \pm$

$0.44_{-0.47}^{+0.73}) \times 10^{-4}$, where the errors are statistical, systematic and model-dependence. The model-dependence is derived from the 1σ error ellipse for the $m_b\text{-}\mu_\pi^2$ fit. The central value in the shape function scheme is reduced to 4.55×10^{-4} if the Gaussian form is used.

Finally the sample is divided into b and \bar{b} decays using the charge of the lepton tag to measure $A_{CP}(B \rightarrow X_{s+d}\gamma) = \frac{N^+ - N^-}{N^+ + N^-} \frac{1}{1 - 2\omega}$ where $N^{+(-)}$ are the positively (negatively) tagged signal yields and $1/(1 - 2\omega)$ is the dilution factor due to the mistag fraction ω . A requirement $2.2 < E_\gamma^* < 2.7$ GeV maximizes the statistical precision of the measurement as determined from simulated data. The yields are $N^+ = 349 \pm 48$ and $N^- = 409 \pm 45$. The bias on A_{CP} due to any charge asymmetry in the detector or $B\bar{B}$ background is measured to be -0.005 ± 0.013 using control samples of $e^+e^- \rightarrow X\gamma$ and $B \rightarrow X\pi^0, \eta$. The mistag fraction due to mixing is $9.3 \pm 0.2\%$ [19]. An additional $2.6 \pm 0.3\%$ mistag fraction arises from leptons from D decay, π^\pm faking μ^\pm , γ conversions, π^0 Dalitz decay, and charmonium decay. After correcting for charge bias and dilution $A_{CP} = -0.110 \pm 0.115(\text{stat.}) \pm 0.017(\text{syst.})$, including multiplicative systematic uncertainties from the $B\bar{B}$ background subtraction (5.4%) and the dilution factor (1.0%). The model-dependence uncertainty due to differences in the $B \rightarrow X_s\gamma$ and $B \rightarrow X_d\gamma$ spectra is estimated to be negligible.

In conclusion, the branching fraction and the energy moments of the photon spectrum in $B \rightarrow X_s\gamma$ are measured for $E_\gamma > 1.9$ GeV. The moments are consistent with previous measurements [10, 11, 12] and are used to extract values of m_b and μ_π^2 which are consistent with those extracted from semi-leptonic B decays [20]. These measurements have been used to reduce the systematic error in the estimation of $|V_{cb}|$ and $|V_{ub}|$ [7]. The measured branching fractions are in agreement with the SM expectation and previous measurements. The measured A_{CP} is also consistent with the SM expectation.

We are grateful for the excellent luminosity and machine conditions provided by our PEP-II colleagues, and for the substantial dedicated effort from the computing organizations that support BABAR. The collaborating institutions wish to thank SLAC for its support and kind hospitality. This work is supported by DOE and NSF (USA), NSERC (Canada), IHEP (China), CEA and CNRS-IN2P3 (France), BMBF and DFG (Germany), INFN (Italy), FOM (The Netherlands), NFR (Norway), MIST (Russia), MEC (Spain), and PPARC (United Kingdom). Individuals have received support from the Marie Curie EIF (European Union) and the A. P. Sloan Foundation.

* Also at Laboratoire de Physique Corpusculaire, Clermont-Ferrand, France

† Also with Università di Perugia, Dipartimento di Fisica, Perugia, Italy

‡ Also with Università della Basilicata, Potenza, Italy

- [1] T. Hurth, Rev. Mod. Phys. **75**, 1159 (2003) and references therein.
- [2] T. Hurth, E. Lunghi and W. Porod Nucl. Phys. B **704**, 56 (2005) and references therein.
- [3] P. Gambino, Nucl. Phys. B Proc. Suppl. **156**, 169 (2006) and references therein.
- [4] A.L. Kagan and M. Neubert, Eur. Phys. J. C **7**, 5 (1999).
- [5] D. Benson, I.I. Bigi and N. Uraltsev, Nucl. Phys. B **710**, 371 (2005).
- [6] B.O. Lange, M. Neubert and G. Paz, Phys. Rev. D **72**, 073006 (2005).
- [7] O. Buchmüller and H. Flächer Phys. Rev. D **73**, 073008 (2006); BABAR collaboration, B. Aubert *et al.*, Phys. Rev. D **73**, 012006 (2006).
- [8] J.M. Soares, Nucl. Phys. B **367**, 575 (1991); T. Hurth and T. Manuel, Phys. Lett. B **511**, 196 (2001).
- [9] CLEO Collaboration, T.E. Coan *et al.*, Phys. Rev. Lett. **86**, 5661 (2001); BABAR Collaboration, B. Aubert *et al.*, Phys. Rev. Lett. **93**, 021804 (2004); BELLE Collaboration, S. Nishida *et al.*, Phys. Rev. Lett. **93**, 031803 (2004).
- [10] CLEO Collaboration, S. Chen *et al.*, Phys. Rev. Lett. **87**, 251807 (2001).
- [11] BELLE Collaboration, P. Koppenburg *et al.*, Phys. Rev. Lett. **93**, 061803 (2004).
- [12] BABAR Collaboration, B. Aubert *et al.*, Phys. Rev. D **72**, 052004 (2005).
- [13] BABAR Collaboration, B. Aubert *et al.*, Nucl. Instrum. Methods A **479**, 1 (2002).
- [14] GEANT4 Collaboration, D. Agostinelli *et al.*, Nucl. Instrum. Methods A **506**, 250 (2003).
- [15] D. J. Lange, Nucl. Instrum. Meth. A **462**, 152 (2001).
- [16] ‘PYTHIA 5.7 and JETSET 7.4: Physics and manual’, by T. Sjöstrand (Lund U.), hep-ph/9508391.
- [17] BABAR Collaboration, B. Aubert *et al.*, hep-ex/0409047 and hep-ex/0408075.
- [18] CKMfitter Group (J. Charles *et al.*), Eur. Phys. J. C **41**, 1 (2005).
- [19] Particle Data Group, S. Eidelman *et al.*, Phys. Lett. B **592**, 1 (2004).
- [20] BABAR Collaboration, B. Aubert *et al.*, Phys. Rev. Lett. **93**, 011803 (2004).

Appendix

The correlation matrices for the statistical, systematic and model-dependence errors of the first and second moments are given in tables II, III and IV respectively. The matrices are symmetric so only the upper half is tabulated. The moments are measured for four energy ranges, $1.9, 2.0, 2.1, 2.2 < E_\gamma < 2.7$ GeV.

